A Two-Element Circularly-Polarized Antenna Array for UHF-Band RFID Reader Applications

Joung-Min Park[1] · Yun-Mi Kim[1] · Bierng-Chearl Ahn[1] · Chan-Sik Park[1] · Eun-Jong Cha[2]

Abstract

In this paper, we present a two-element circularly-polarized antenna array for UHF-band RFID reader applications. The antenna element in the array is a corner-truncated rectangular patch placed on a thick plastic-foam dielectric. The patch is fed on one of its edges by a microstrip line printed on a separate thin substrate. The array antenna is fed by a microstrip power divider. Parametric studies on the patch are carried out, from which an optimum design of a single antenna element is derived. The element spacing and the feed network of the array are investigated. A commercial electromagnetic software is employed in the analysis and design of the antenna. The designed array is fabricated and tested. Measurements show good performance characteristics of the fabricated antenna: a 11.2-dBi gain, a reflection coefficient of −14 dB, an axial ratio less than 3 dB over 3-dB beamwidths of 40 and 60 degrees on two principal planes.

Key words : RFID Reader Antenna, Circularly-Polarized Antenna, Patch Array Antenna.

Ⅰ. Introduction

Intensive research and development efforts in RFID technologies have been made all over the world in the last few years, which are expected to be continued considering current market needs. The RFID reader antenna is one of important components in an RFID system and has been investigated by many researchers[1]~[3]. The standard 6-dBi gain antenna is widely used in the RFID tag reader. The current Korean standard on the 900-MHz band RFID system calls for an effective isotropically radiated power (EIRP) less than 4 W. If the power input to the reader antenna is 1 W, the antenna gain should thus be less than 6 dBi. Antennas with a higher gain and a narrower beamwidth, however, are useful for applications where it is necessary to read a tag over a narrower range of angles using a correspondingly reduced transmitter power or where it is required to extend the tag read range provided that the 4-W EIRP restriction is not applicable. Antenna arrays for RFID applications have been actively investigated in recent years[4]~[6].

For RFID reader applications, compact and lightweight antennas are preferable for obvious reasons of the space economy. Thus thick antennas such as the helix and the horn are not suitable for RFID reader applications. In this paper we present a two-element array of circularly-polarized rectangular patches for UHF-band(908.5~914.0 MHz in Korea) RFID reader applications. The bandwidth of the UHF RFID system is in effect very narrow(5.5 MHz). We, however, have selected an antenna structure with a bandwidth wide enough so that large manufacturing tolerances could be accommodated for the low-cost production. The antenna element employed in out study is a modified form of the wideband circularly-polarized patch proposed by Chang and co-workers in 2003[7].

In the Chang's patch[7] shown in Fig. 1, the distance from the ground plane to the patch is greatly increased up to 0.2 times the free-space wavelength in order to increase the bandwidth. The patch is fed on one of edges by a coaxial probe through a vertical ground plane which is an extension of the horizontal ground plane. In this case, the probe length can be made small minimizing the probe inductance. With this scheme, Chang and co-workers were able to achieve a circular-polarization bandwidth of about 10 %.

In this paper, detailed parametric studies on the Chang's patch are given for the first time. The coaxial probe feeding the patch is replaced by a microstrip line, which enables a compact realization of the array feed network in a printed circuit form. It would be far more complicated if one tries to implement the array feed network using coaxial transmission lines. A plastic foam dielectric is used to support the patch.

Firstly we present the design and measurement of a single patch element. Parametric studies on a patch were

Manuscript received October 25, 2005 ; revised January 20, 2006. (ID No. 20051025-042J)

[1]School of Electrical and Computer Engineering, Chungbuk University, Cheongju, Korea.
[2]School of Medicine, Chungbuk University, Cheongju, Korea.

carried out using the Microwave Studio®, a widely-used commercial software for the numerical analysis of electromagnetic field and wave problems. Next we investigated the design of a two-element array of patch elements. The spacing between elements was optimized for a maximum gain. The array feed network was implemented in the form of a microstrip power divider on an FR-4 printed circuit board. Performances of the fabricated array were measured and compared to MWS® simulations.

Ⅱ. Antenna Design, Fabrication and Measurements

2-1 Design of a Single Antenna Element

The design of the circularly-polarized patch has been studied by numerous researchers[8]~[13]. The circular-polarization bandwidth of a patch antenna realized on a thin dielectric substrate is only a few percent at maximum. In 2003, Chang and co-workers proposed a new form of a circularly-polarized patch[7] shown in Fig. 1, where the coordinate system and design parameters are shown. The patch is of a square shape(W=L) with a length of about 0.35~0.45 times the free-space wavelength[7] depending on the distance from the ground plane to the patch. With a large distance between the ground plane and the patch, the resonant length of the patch is significantly reduced from a half wavelength because of large fringing effects at the patch's radiating edges[7]. A circularly-polarized radiation is obtained by truncating two opposite corners of the patch in an appropriate amount to excite two orthogonal near-degenerate resonant modes in phase quadrature.

The space between the patch and the ground plane is filled with the air, and the patch is supported by low-dielectric constant plastic posts. The bandwidth is enhanced by increasing the distance from the ground plane to the patch and by feeding the patch on the edge via the vertical ground plane. The probe length can be made small by placing the patch close to the vertical ground plane, resulting in a small probe inductance. If the patch is fed from beneath the patch via the horizontal ground plane, the probe length will be large, which leads to a large probe inductance severely deteriorating the impedance match. To begin with an optimum design of a single element in the array, firstly we performed parametric studies on the Chang's patch. Next we modified the Chang's patch by using the plastic foam dielectric and the microstrip feed.

The single antenna element is designed using the well-known commercial software Microwave Studio(MWS)® by Compute Simulation Technologies(CST). The initial value of the patch length is determined from the following equation.

$$L=\frac{\lambda}{2}-2\Delta L \tag{1}$$

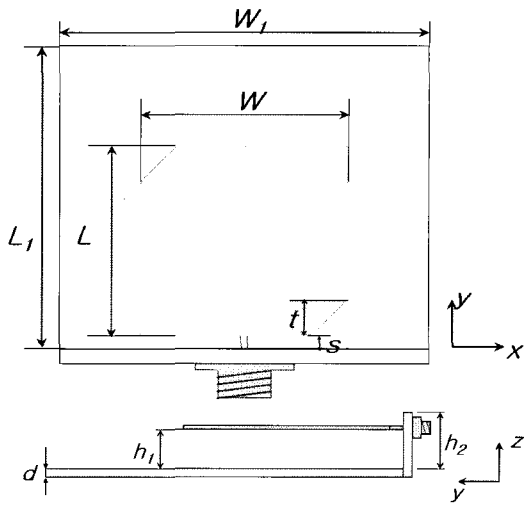

Fig. 1. Structure, parameters and the coordinate system of the single antenna element.

$$\Delta L=0.412h\frac{(\varepsilon_{r,eff}+0.3)(W/h+0.264)}{(\varepsilon_{r,eff}+0.258)(W/h+0.8)} \tag{2}$$

where $\varepsilon_{r,eff}$=1, $\lambda=c/f$, W is the patch width, and h(=h_1) is the distance from the ground plane to the patch. The distance(h_1) from the ground plane to the patch can range from 0.05 to 0.15 times the wavelength. The larger h_1, the larger the bandwidth. In this paper, we let h_1=20 mm(0.06 λ) in order to make the antenna compact. Initially assuming W=0.45 λ, we obtain L=149 mm using Eq. (1).

Fig. 2 shows the reflection coefficient of the patch for various patch lengths. Some typical values were assigned to other parameters of the patch. We observe in Fig. 2 that larger patches resonate at lower frequencies as expected. The patch resonates at 912 MHz with W=L=140 mm=

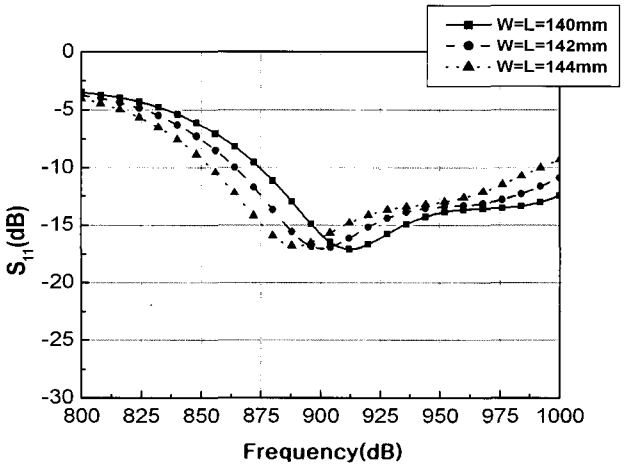

Fig. 2. Reflection coefficient of the patch for various values of the patch length L(W_1=235, L_1=215, t=31, s=7, h_1=20, h_2=26, d=2 mm).

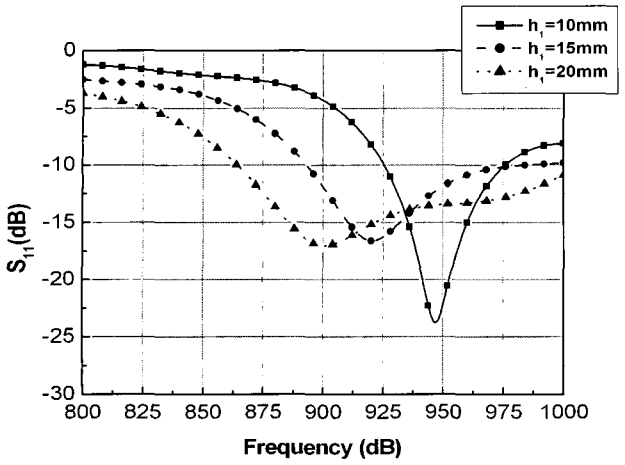

Fig. 3. Reflection coefficient of the patch for various values of the dielectric height h_1(W_1=235, L_1= 215, t=31, s=7, W= L=141, h_2=26, d=2 mm).

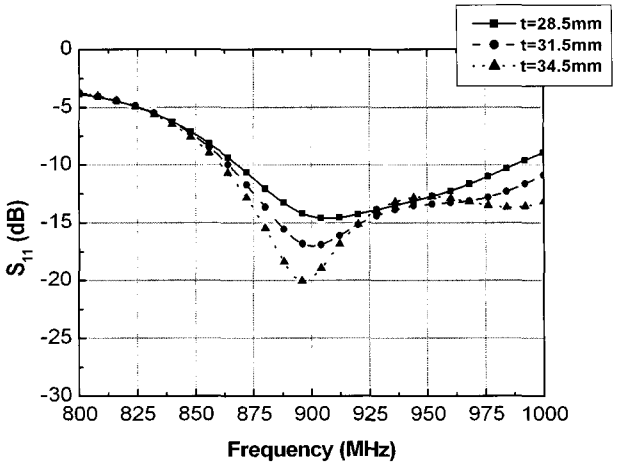

Fig. 5. Effect of the truncation t on the patch reflection coefficient(W_1=235, L_1=215, h_1=20, s=7, W= L=141, h_2=26, d=2 mm).

0.42 λ . Fig. 3 shows the reflection coefficient of the patch for various values of the distance(h_1) from the ground plane to the patch. We observe that smaller values of h_1 lead to a higher resonant frequency and a smaller bandwidth.

Next we determined the optimum value of the patch truncation t. Fig. 4 shows the axial ratio for various values of the patch truncation. With a patch truncation larger than the optimum value, the axial ratio and the resonant frequency are increased. Truncation of the patch leads to the increase in the resonant frequency which is given approximately by [8]

$$f_r' = \frac{f_r}{\left(1-\frac{2\Delta S}{S}\right)} \tag{3}$$

where ΔS is the truncation area, S is the patch area before truncation, and f_r' and f_r are the resonant frequencies after and before truncation, respectively. Fig. 5 shows the effect of the truncation on the reflection coefficient of the patch. We observe that the truncation affects the input impedance of the patch rather significantly.

The input impedance of the patch is sensitively dependent upon the gap s between the vertical ground plane and the patch edge. It is depicted in Fig. 6, where the reflection coefficient of the patch is shown for various values of s. The best performance over 908.5~914.0 MHz is obtained when s is 7 mm.

Finally we investigated the effect of the ground plane size on the antenna performance. Figs. 7 and 8 show variations of the reflection coefficient and the axial ratio versus the width of the ground plane. The reflection coefficient

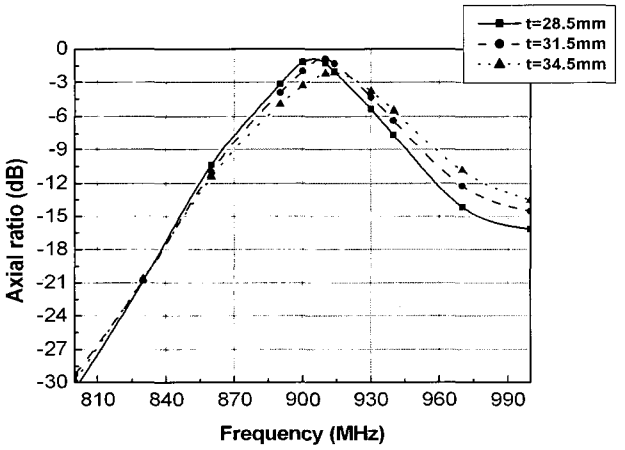

Fig. 4. Dependence of the axial ration on the patch truncation t (W_1=235, L_1=215, h_1=20, s=7, W= L=141, h_2=26, d =2 mm).

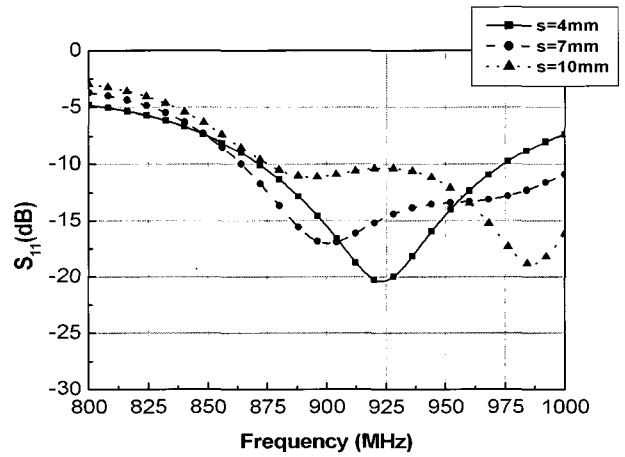

Fig. 6. Effect of the ground-to-patch gap s on the patch reflection coefficient(W_1=235, L_1=215, h_1=20, t= 31, W= L=141, h_2=26, d=2 mm).

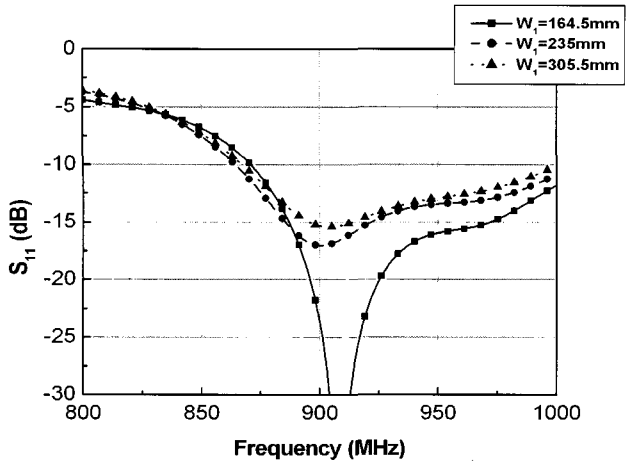

Fig. 7. Effect of the ground plane width W_1 on the patch reflection coefficient(L_1=215, h_1=20, t=31, $W=L$ =141, h_2=26, d=2 mm).

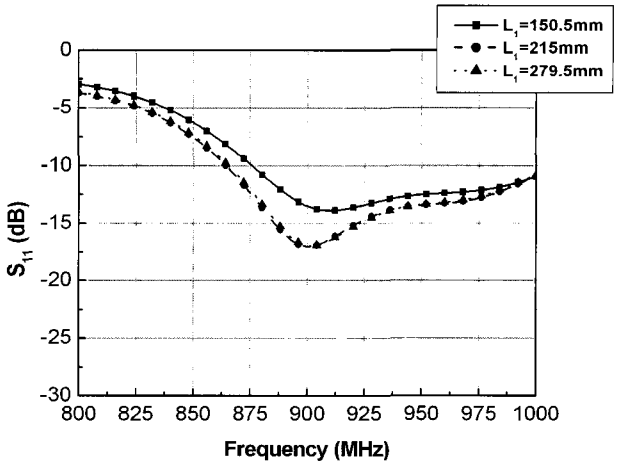

Fig. 9. Effect of the ground plane length L_1 on the patch reflection coefficient(W =235, h_1=20, t=31, $W=L$=141, h_2=26, d=2 mm).

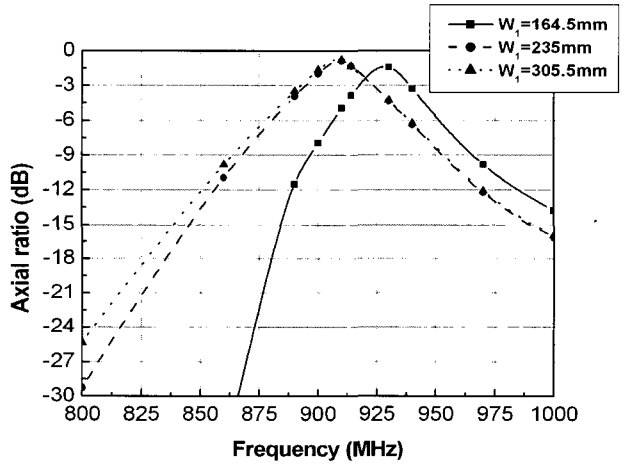

Fig. 8. Effect of the ground plane width W_1 on the axial ratio(L_1=215, h_1=20, t=31, $W=L$=141, h_2= 26, d=2 mm).

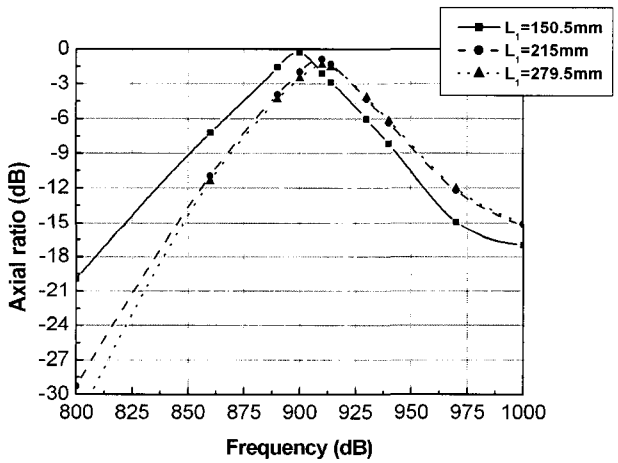

Fig. 10. Effect of the ground plane length L_1 on the axial ratio(W =235, h_1=20, t= 31, $W=L$=141, h_2=26, d= 2 mm).

and the axial ratio are changed when the ground plane width W_1 is reduced to a small value. With a small value of the ground plane width, the frequency for an optimum axial ratio is increased. From Figs. 7 and 8, we find that the patch performance is minimally affected with a ground plane width of 235 mm.

Figs. 9 and 10 show variations of the reflection coefficient and the axial ratio versus the length L_1 of the ground plane. Similar observations can be made regarding effects of the ground plane length. With a small value of the ground plane length, the frequency for an optimum axial ratio is reduced. From Figs. 9 and 10, we observe that a ground plane length of 215 mm minimally affects the patch performance.

After many design iterations, we finally obtained optimum values of the patch dimension: W_1=235, L_1=215, $W=L$=141, t=31, s=7, h_1=20, h_2=26, d=2(all in mm). The patch is fed by an 1.2-mm diameter probe of an SMA connector, where a Teflon(ε_r=2.08) with a diameter of 4.2 mm is placed between the inner and outer conductors for a 50-ohm characteristic impedance.

Fig. 11 shows the fabricated antenna where a plastic foam with a low dielectric constant(ε_r=1.03) is employed to support the patch above the ground plane. Figs. 12～15 show measured antenna performances along with the simulation. Fig. 12 shows the reflection coefficient versus the frequency of the fabricated antenna, where a good agreement between the simulation and the measurement

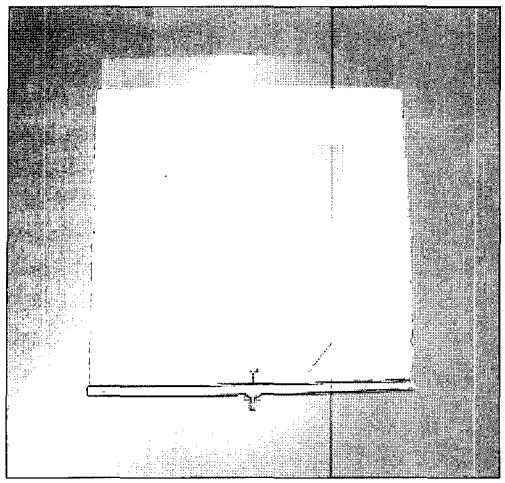

Fig. 11. Photograph of the fabricated patch antenna.

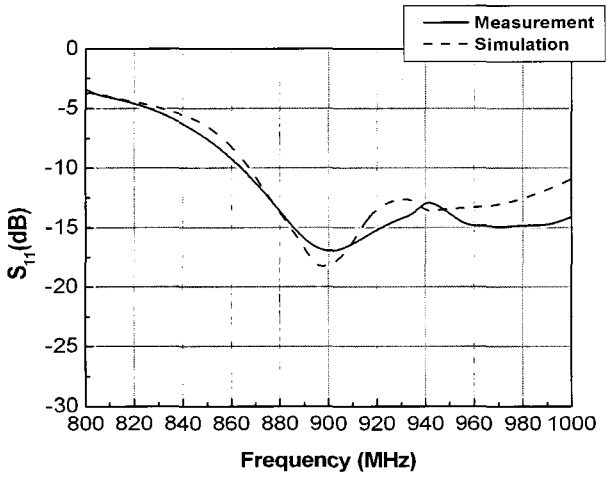

Fig. 12. Reflection coefficient versus the frequency of the fabricated patch antenna.

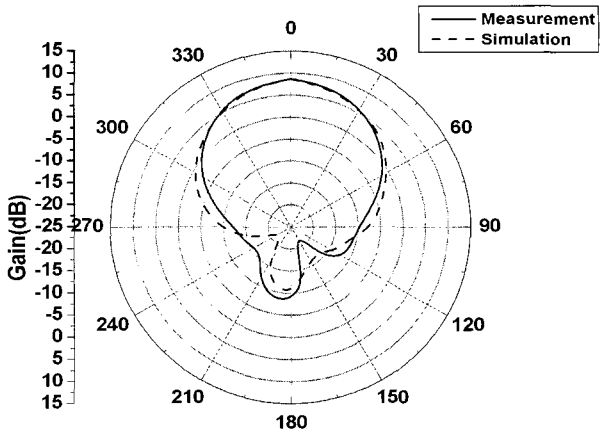

(a) On zx-plane

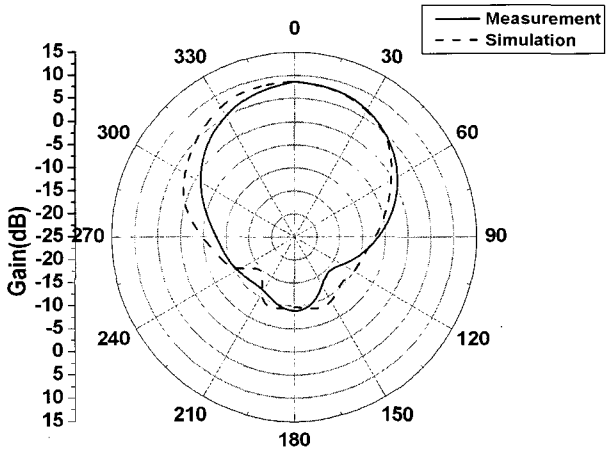

(b) On yz-plane

Fig. 13. Gain pattern at 910 MHz of the fabricated patch antenna.

can be observed. The fabricated antenna has a reflection coefficient less than -15 dB over 908.5~914.0 MHz.

Fig. 13 shows the gain pattern at 910 MHz of the fabricated antenna. The zero-degree angle corresponds to the direction normal to the patch surface. The gain pattern was measured by the cylindrical near-field probing method, where the absolute gain was compared with that of a standard-gain horn antenna. The agreement between the simulation and the measurement is good. Antenna beamwidths are about 60 and 70 degrees in zx- and yz-planes, respectively.

Fig. 14 shows the axial-ratio pattern at 910 MHz of the fabricated antenna, where negative values of the axial ratio is used for graphical convenience whereas the normal definition of the axial ratio gives only positive values. The axial ratio was obtained by near-field probing horizontal and vertical components of the electric field vector radiated from the antenna and calculating the axial ratio using the formula given in [14]. We observe in Fig. 14 that the absolute value of the axial ratio is less than 3 dB over half-power beamwidth angles.

Fig. 15 shows the gain versus of the fabricated antenna versus the frequency. The antenna gain is 8.5~8.8 dBi over 900~914 MHz. Fig. 16 shows the axial ratio at $\theta = 0°$ of the fabricated antenna versus the frequency. The absolute value of the axial ratio at $\theta = 0°$ is less than 2.5 dB over 908.5~914.0 MHz.

2-2 Design of a Two-Element Array

Employing the wideband circularly-polarized patch element described in Section 2-1, we designed a two-element array antenna. Firstly we determined the element spacing for a maximum gain. Fig. 17 shows the gain of the array

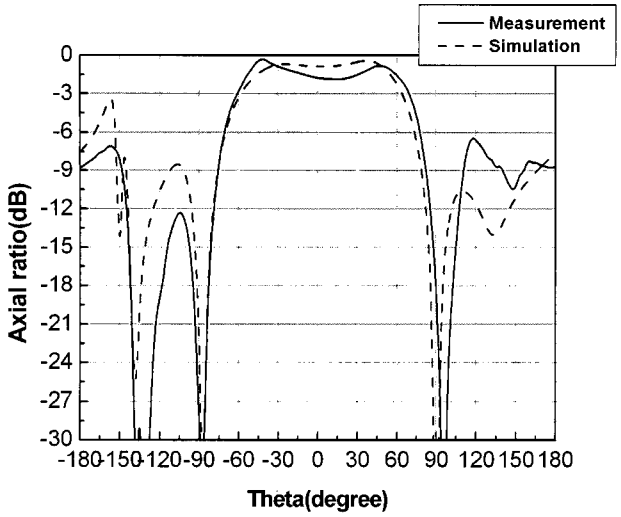

(a) On *zx*-plane

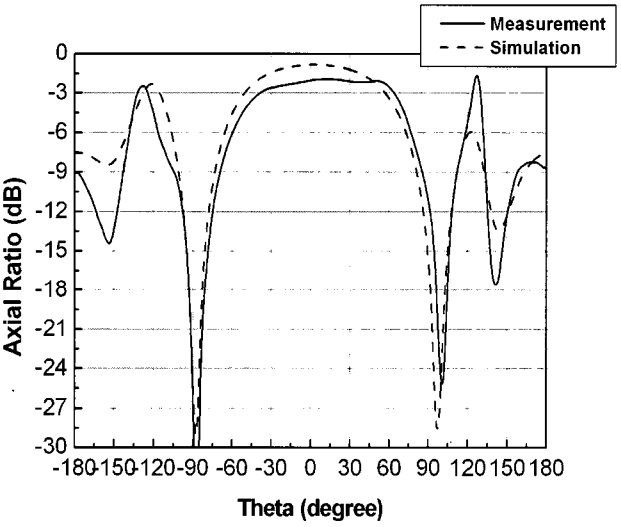

(b) On *yz*-plane

Fig. 14. Axial ratio at 910 MHz of the fabricated patch antenna.

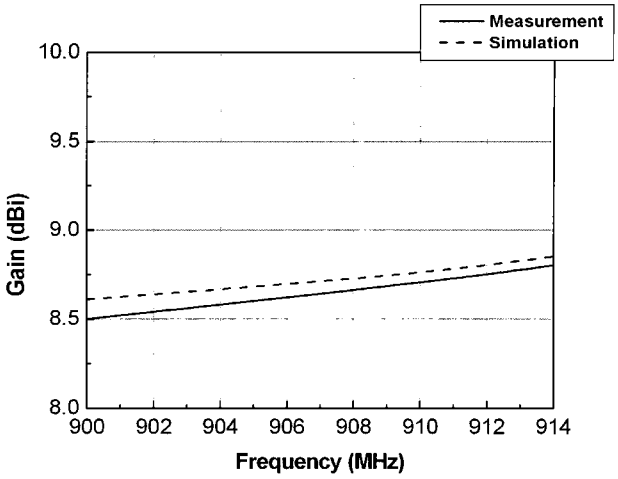

Fig. 15. Gain of the fabricated patch antenna element versus the frequency.

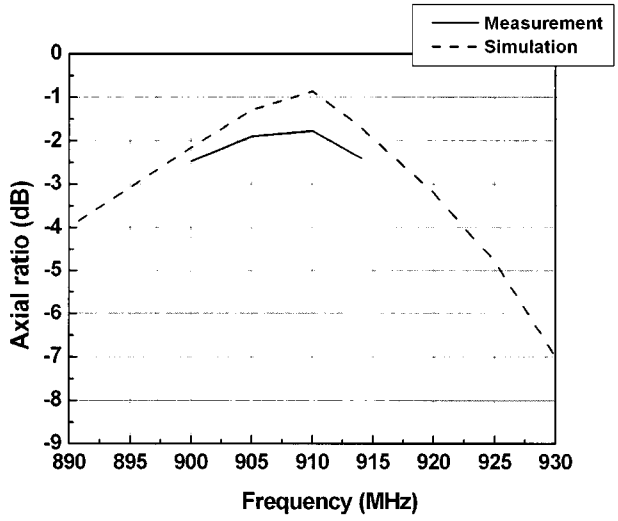

Fig. 16. Axial ratio at θ =0° of the fabricated patch antenna element versus the frequency.

versus the element spacing, which is obtained using the array utility in MWS® where the array gain is calculated from the element radiation pattern and the element spacing. The maximum gain is 12.6 dBi and occurs when the element spacing is 0.7 times the wavelength. The loss of the feed network is not taken into account in this calculation. The result of Fig. 17 was employed in setting the initial value of the element spacing when the array antenna including the feed network was optimized using MWS®.

The next step in the development of the array is to design the feed network. The feed network is most conveniently realized in the form of a microstrip circuit. The coaxial probe feeding the single element described in Section 2.1 is now replaced by a microstrip line and the vertical ground plane of Fig. 1 is modified to accommodate a printed circuit board(compare Fig. 19 with Fig. 1). With this modification of the feed geometry, the input impedance of the patch now is increased to about 120 ohms, while with a coaxial feed it is 73 ohms.

The reflection coefficient to be realized is set to be − 15 dB satisfying − 10 dB value in antenna specifications to ease the implementation of the feed network. For a − 15 dB reflection coefficient with a 50-ohm reference impedance, the input impedance of the feed network can be either 35 ohms or 72 ohms. The value of 35 ohms can be more conveniently realized by combining two 70-ohm impedances using a microstrip power combiner shown in Fig. 18.

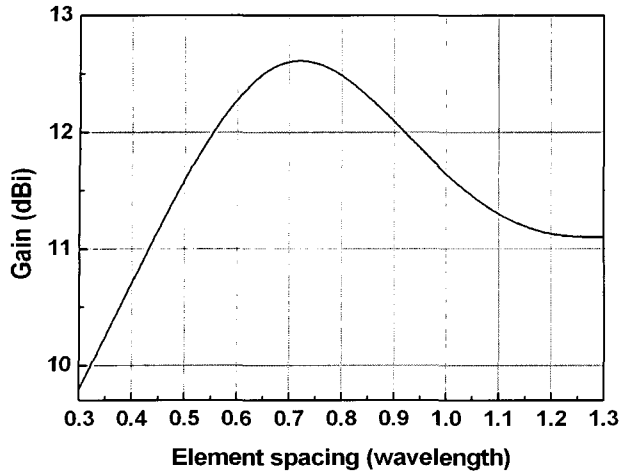

Fig. 17. Gain of the array versus the element spacing.

A perfect impedance match is possible when the input impedance of the feed network is 50 ohms. In this case, however, widths of the microstrip line become small and one will face with problems of manufacturing tolerances and the mechanical strength of the microstrip line. With the input impedance of the feed network being 35 ohms, these problems are rendered less severe.

Fig. 18 shows the topology of the feed network. The 120-ohm input impedance(Z_p) of a single patch is transformed to 70 ohms(Z_1) using a quarter-wave impedance transformer with a characteristic impedance of 92 ohms (Z_2) according to the following formula.

$$Z_2 = \sqrt{Z_1 Z_p} \tag{4}$$

The 92-ohm line is realized by a microstrip of width 0.54 mm on the 1-mm thick FR-4 substrate with a dielectric constant of 4.3 and a loss tangent of 0.02. A thinner line is required if one transforms the 120-ohm patch impedance to 100 ohms, which leads to a tighter manufacturing tolerance and weaker mechanical strength.

Finally in Fig. 18, we have Z_2=92 ohms, Z_1=70 ohms (strip width=1.03 mm) and Z_0=50 ohms(strip width=1.92 mm), where the array input impedance Z_{in} seen at the power divider junction is 35 ohms as given by

$$Z_{in} = Z_1 / 2 \tag{5}$$

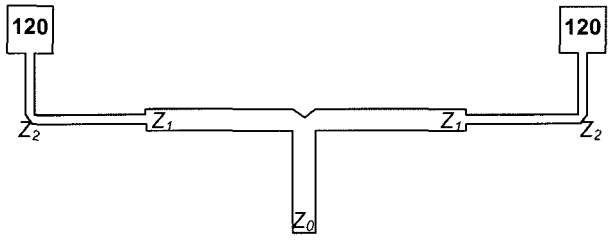

Fig. 18. Topology of the microstrip feed network.

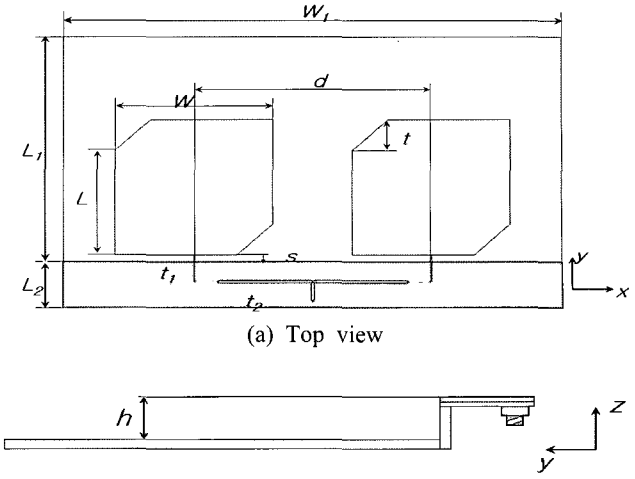

(a) Top view

(b) Side view

Fig. 19. Structure and parameters of the antenna array.

Fig. 19 shows the entire structure and parameters of the antenna array. The overall structure was simulated using MWS® to obtain parameter values of the finally designed array: W_1=445.5, L_1=234.7, L_2=48, W=L=141, d=211.5, s=7, t=32, h=20 mm. The width of a short section of a strip feeding the patch is 1.3 mm.

The element spacing is optimized to be 0.63 λ close to 0.70 λ given by the array simulator module(see Fig. 17). The optimum element spacing is determined by analyzing the entire array structure including the microstrip feed network, where the actual ground plane size, the mutual coupling between two elements, and the interaction between the patch and the microstrip feed line are taken into account. The 0.70- λ spacing in Fig. 17 was obtained

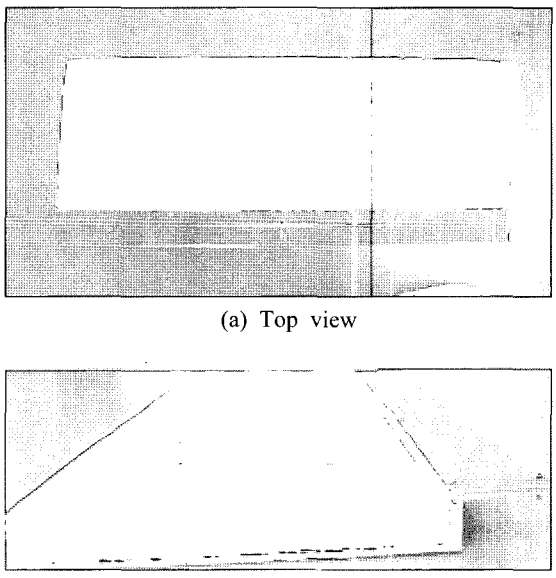

(a) Top view

(b) Side view

Fig. 20. Fabricated antenna array.

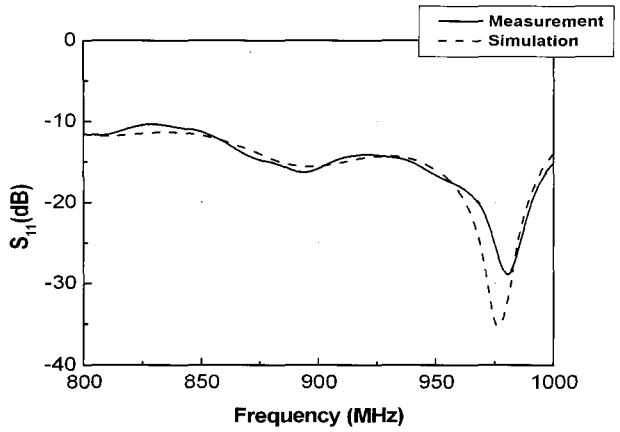

Fig. 21. Reflection coefficient of the fabricated antenna array versus the frequency.

simply from the element pattern and the element distance.

The designed antenna was fabricated where a plastic foam material with a dielectric constant of 1.03 was used to support patch elements realized using the copper film. The microstrip feed network was printed on an 1-mm thick FR-4 substrate. As an output interface, an SMA connector was attached to the output of the feed network at the back of the ground plane. Fig. 20 is a photograph of the fabricated antenna.

Figs. 21~24 show measured performances of the fabricated array antenna. Fig. 21 shows the reflection coefficient of the antenna, where we observe a reflection coefficient less than -14 dB over 908.5~914.0 MHz. Fig. 22 shows gain patterns on the horizontal(zx) and vertical(yz) planes, where we observe a good agreement between the simulation and the measurement. Gain patterns were measured using the same method as used in the measurement of a single element. Beamwidths are 40 and 60 degrees on zx- and yz-planes respectively.

Fig. 23 shows the axial ratio pattern, where we observe that the axial ratio is less than 3 dB over the antenna

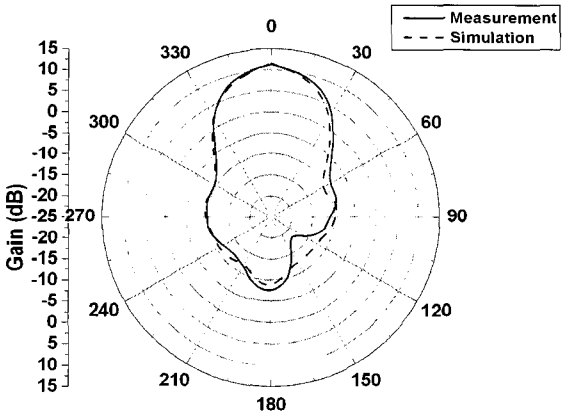

(a) on zx-plane

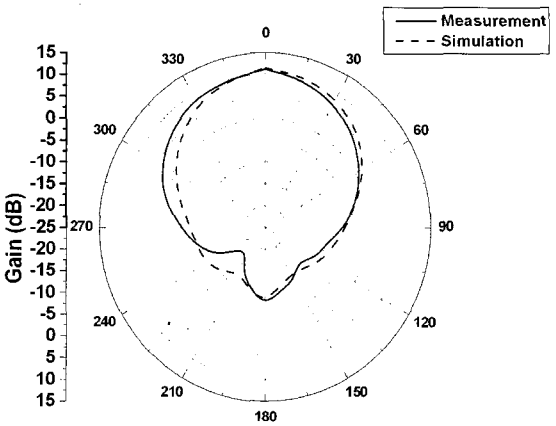

(b) on yz-plane

Fig. 22. Radiation pattern at 910 MHz of the fabricated antenna array.

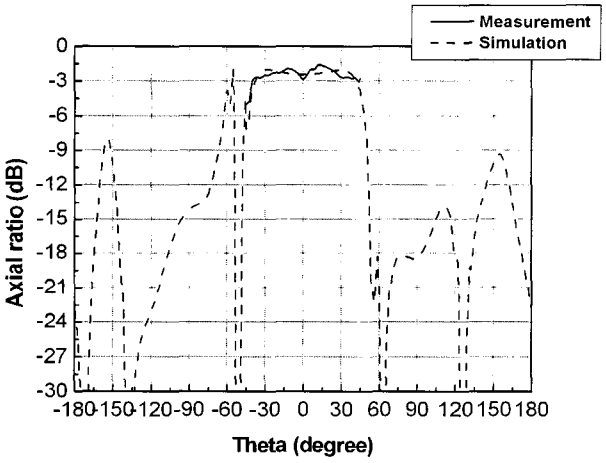

(a) On zx-plane

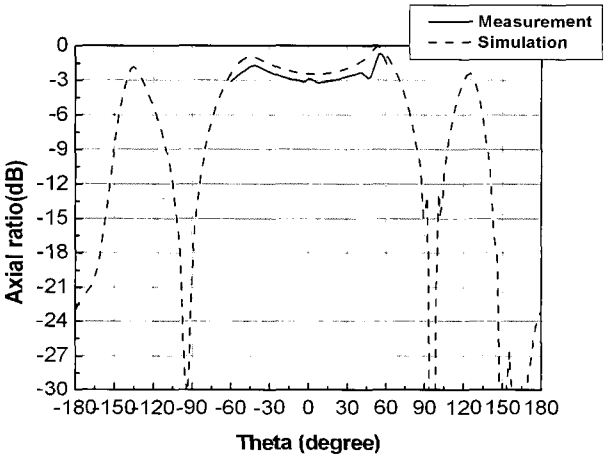

(b) On yz-plane

Fig. 23. Axial ratio at 910 MHz of the fabricated antenna array.

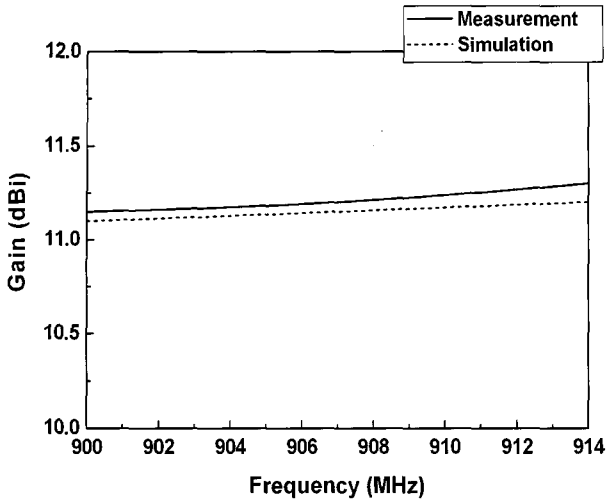

Fig. 24. Gain versus the frequency of the fabricated antenna array.

beamwidth. The axial ratio was measured using the same method as used in the measurement of a single element. Fig. 24 shows the gain versus the frequency. The measured gain is 11.2~11.3 dBi over 908.5~914.0 MHz and is slightly larger than the simulated value, which is believed to be due to measurement errors.

The total loss of the feed network is estimated to be about 1.3 dB(74 % efficiency). Fig. 24 shows the axial ratio at $\theta = 0°$ versus the frequency of the fabricated antenna array. The absolute value of the axial ration is less than 3 dB over 908.5~914.0 MHz.

As a check on the antenna performance in the field, we investigated the tag read range of the fabricated antenna. The test was done using the RFID system by the Alien

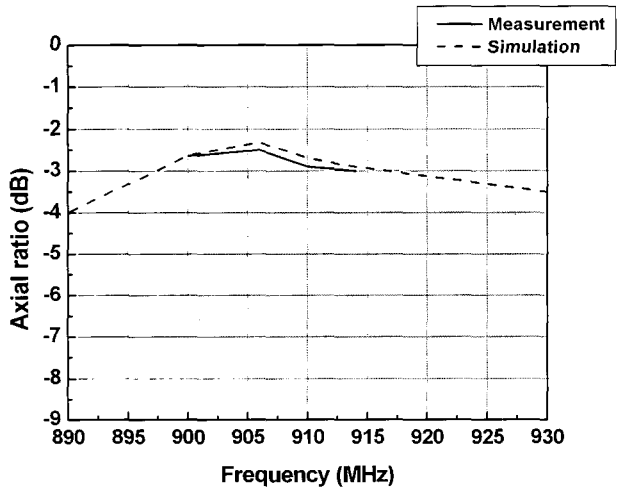

Fig. 25. Axial ratio at θ=0° of the fabricated antenna array versus the frequency.

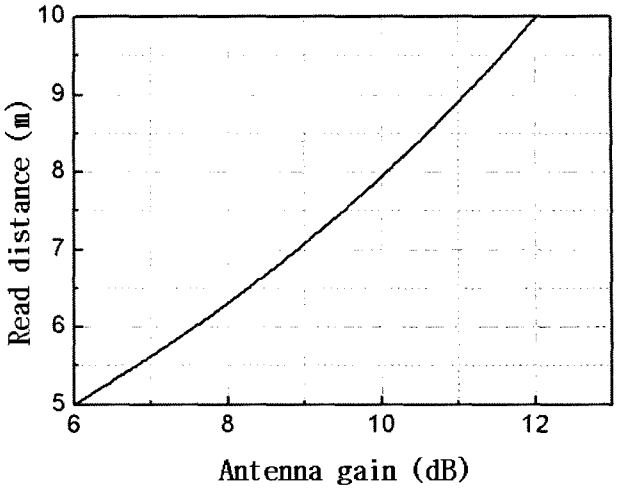

Fig. 26. Tag read range versus the reader antenna gain.

Company with the transmitted power of one watt and the EPC Class1 UHF RFID Tag(64 bit) "Squiggle T". The gain of the Alien's reader antenna is 6.0 dBi. The read range R can be calculated using the Friis transmission formula[15]

$$R = \frac{\lambda}{2\pi}\sqrt{\frac{P_t G_t G_r \tau}{P_{th}}} \tag{6}$$

where λ is the wavelength, P_t is the power transmitted by the reader, G_t is the gain of the reader antenna, G_r is the gain of the tag, P_{th} is the minimum threshold power necessary to provide enough power to the RFID tag chip, and τ is the power transmission coefficient of the tag. When all other parameters are kept constant, the read range is proportional to the square root of the reader antenna gain. The measured read range of the Alien's reader antenna is 5 meters, from which the graph in Fig. 26 is generated using Eq. (6).

The tag read range of the fabricated array antenna was measured to be 9.6 meters. The graph in Fig. 26 yields a read range of 9.1 meters. From the tag read range experiment, we confirmed the increased read range of the proposed antenna.

Ⅲ. Conclusions

In this paper, we proposed an RFID reader antenna array consisting of two circularly-polarized patches and operating at 908.5~914.0 MHz. The antenna is of simple construction and can be economically fabricated using low cost materials. Firstly we presented methods and results of the optimum design of a single patch element obtained by modifying the patch proposed by Chang and co-workers. Secondly we presented an array of two patch elements spaced 0.63 λ apart and fed by a microstrip feed network. Measurements of the fabricated antenna showed good

antenna performances: 11.2 dBi gain, beamwidths of 40 and 60 degrees on the horizontal and vertical planes, axial ratio less than 3 dB, reflection coefficient less than − 14 dB. The maximum RFID tag read range of the fabricated antenna with an 1-W transmitted power was measured to be 9.6 meters, which is a substantial improvement over the 5-m read range of the commercial 6-dBi gain antenna. The proposed antenna can be used in extending the read range of the standard RFID reader antenna operating at the UHF band when the 1-W EIRP restriction is not applicable or in narrowing the angular range of the tag identification.

This work was supported by the Regional Research Centers Program of the Ministry of Education & Human Resources Development in Korea.

References

[1] X. Qing, N. Yang, "2.45 GHz circularly polarized RFID reader antenna", *Proc. IEEE 9th Int. Conf. Comm. Sys.*, pp. 612-615, Sep. 2004.

[2] P. R. Foster, R. A. Burberry, "Antenna problems in RFID systems", *Proc. IEE Colloquium on RFID Technology*, pp. 3/1-3/5, Oct. 1999.

[3] P. Raumonen, M. Keskilammi, L. Sydangeimo, and M. Kivikoski, "A very low profile CP EBG antenna for RFID reader", *Dig. 2004 IEEE Antennas Propagat. Soc. Int. Symp.*, pp. 3808-3111, Jun. 2004.

[4] S. K. Padhi, N. C. Karmakar, and C. L. Law, "Dual polarized reader antenna array for RFID application", *Dig. 2003 IEEE Antennas Propagat. Soc. Int. Symp.*, pp. 265-268, Jun. 2003.

[5] P. Salonen, M. Kesilammi, L. Syddanheimo, and M. Kovikoski, "An intelligent 2.45 GHz multi-dimensional beam-scanning X-array for modern RFID reader", *Dig. 2000 IEEE Antennas Propagat. Soc. Int. Symp.*, pp. 190-193, Jul. 2000.

[6] P. Salonen, L. Syddanheimo, "A 2.45 GHz digital beam-forming antenna for RFID reader", *Proc. IEEE 55th Vehicular Tech. Conf.*, pp. 1766-1770, May 2002.

[7] F. -S. Chang, K. -L. Wong, and T. -W. Chiou, "Low-cost broadband circularly polarized patch antenna", *IEEE Trans. Antennas Propagat.*, vol. 51, no. 10, pp. 3006-3009, Oct. 2003.

[8] M. Niroojazi, M. N. Azarmanesh, "Practical design of single feed truncated corner microstrip antenna", *Proc. IEEE 2nd Annual Conf. on Communication Networks and Services Research*, pp. 25-29, May 2004.

[9] K.-M. Luk, K.-Y. Hui, "A miniature circularly polarized patch antenna", *Dig. 2003 IEEE Antennas Propagat. Soc. Int. Symp.*, pp. 429-432, Jun. 2003.

[10] M. Fallah-Rad, L. Shafai, "Gain enhancement in linear and circularly polarised microstrip patch antennas using shorted metallic patches", *IEE Proc. Microw. Antennas Propagat.*, vol. 152, no. 3, pp. 138-148, Jun. 2005.

[11] U. Farooq, J. Asad, and H. Jamal, "Design of circularly polarized square microstrip patch antenna", *Proc. IEEE 7th Int. Multi Topic Conf.(INMIC 2003)*, pp. 228-231, Dec. 2003.

[12] W. -S. Chen, "Inset-microstripline-fed circularly polarized microstrip antennas", *Dig. 1999 IEEE Antennas Propagat. Soc. Int. Symp.*, pp. 260-263, Jul. 1999.

[13] N. Herscovici, Z. Sipus, and D. Bonefacic, "Circularly polarized single-fed wide-band microstrip patch", *IEEE Trans. Antennas Propagat.*, vol. 51, no. 6, pp. 1277-1280, Jun. 2003.

[14] C. A. Balanis, *Antenna Theory-Analysis and Design,* 2nd Ed., New York: John Wiley & Sons, pp. 67-68, 1977.

[15] K. V. Seshagiri Rao, P. V. Nikitin, and S. F. Lam, "Antenna design for UHF RFID tags: a review and a practical application", *IEEE Trans. Antennas Propagat.*, vol. 53, no. 12, pp. 3870-3876, Dec. 2005.

Joung-Min Park

received B.E. degree in electrical & computer engineering and the M.E. degree in radio engineering from Chungbuk University in 2004 and 2006, respectively. He is now with Mitto RF Korea Company, Yongin City. His research interests include antennas and microwave circuits.

Yun-Mi Kim

received the B.E. degree in electrical & computer engineering from Chungbuk University in 2005. She is currently working toward the M.E. degree in radio engineering department, Graduate School, Chungbuk University. Her research interests include antennas and microwave circuits.

Bierng-Chearl Ahn

received the B.E. degree in electrical engineering from Seoul National University in 1981, the M.E. degree in electrical engineering form Korea Advanced Institute of Science and Technology in 1983, and the Ph.D. degree in electrical engineering from University of Mississippi in 1992. From 1983 to 1986, he was with Goldstar Precision Company as a research engineer. From 1993 to 1994, he worked for Agency for Defense Development. Since 1995 he has been with Chungbuk University, where he is currently a Professor in the School of Electrical and Computer Engineering. His research interests include applied electromagnetics and antennas.

Chan-Sik Park

received the B.S., M.S. and Ph.D. degrees from the department of control and instrumentation engineering, Seoul University, in February 1984, 1986 and 1997, respectably. He was a Senior Researcher at Samsung Electronics from 1984 to 1997. He is now an Associate Professor at Chungbuk University. His research interest include GNSS and ITS.

Eun-Jong Cha

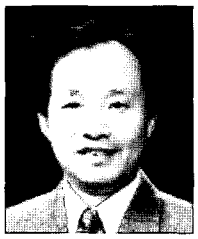

received the B.E. degree in electronics engineering from Seoul National University in 1980, the M.S. and Ph.D. degrees in Medicine form Univesity of Southern California in 1984 and 1987, respectively. Since 1988, he has been with Chungbuk University, where he is currently a Professor in the Department of Medicine. His research interests include medical engineering and the mechanics of human body.